

Eugenol, from *Musa acuminata*, a Potential Antagonist against c-Met in Non-Small Cell Lung Cancer Chemotherapy: *in silico* study

George Oche A., **Sulaiman A. Faoziyat**, Olanrewaju John A., Nwufoh Chika N., Nzikahyel Simon, Adebo Adeola O., Toyin Soyinka., Alakanse Suleiman O. and Seyi Bankole.

Abstract

c-Met (Mesenchymal Epithelial Transition) inhibitors are regarded as a kind of novel drugs in the treatment of non-small cell lung cancer (NSCLC). The current FDA-approved c-Met inhibitors which include crizotinib and cabozantinib have been reported to present an adverse effect when used in NSCLC therapy. This ranges from chest pain, unusual bleeding of the nose and mouth, fever and jaundice. In view of this, research is focus on identifying more potent compounds with no adverse effects that can be used in the treatment of NSCLC.

The aim of this study is to out-source from plant sources (*musa acuminata*) for the best-in-class drug-gable compound via computational tools. For this, twenty-eight (28) chemical compounds (phytochemicals) obtained from *musa acuminata* and retrieved from literatures were screened for their inhibitory effects on c-Met. Eugenol was the lead compound with a binding energy of -5.7.0kcal/mol. Computational docking analysis was performed using PyRx, AutoDock Vina option based on scoring functions and the target was validated so as to ensure that the right target was used for this analysis. These results indicated that eugenol could be one of the potential ligands to treat NSCLC.

Keywords: c-Met, *musa acuminata*, Eugenol

Introduction

Lung cancer is the leading cause of cancer-related death in the world which became a major threat to health and heavy burden for family and society[1,2]. Traditionally, lung cancer is divided into small cell lung cancer (SCLC) and non-small cell lung cancer (NSCLC, accounting for nearly 80% of all lung cancer). Based on histological examination, NSCLC can be further divided into squamous carcinoma, adenocarcinoma and large cell carcinoma. [3]. Even though the underlying mechanism of lung cancer has not been fully elucidated so far, it is widely received that some key genetic mutations in the airway epithelial cells play a pivotal role in the development of this malignancy [4].

All parts of the *musa acuminata* have medicinal applications: the flowers in bronchitis and dysentery and on ulcers; cooked flowers are given to diabetics; the astringent plant sap in cases of hysteria, epilepsy, leprosy, fevers, hemorrhages, acute dysentery and diarrhea, and it is applied on hemorrhoids, insect and other stings and bites; young leaves are placed as poultices on burns and other skin afflictions; the astringent ashes of the unripe peel and of the leaves are taken in dysentery and diarrhea and used for treating malignant ulcers; the roots are administered in

digestive disorders, dysentery and other ailments; *musa acuminata* seed mucilage is given in cases of diarrhea in India [17].

c-MET receptor tyrosine kinase (c-MET RTK) is the receptor for hepatocyte growth factor/scatter factor (HGF/SF) [5]. The mature HGF protein binds to its high-affinity receptor c-MET, leading to its activation and phosphorylation of multiple serine and tyrosine residue sites [6]. The c-MET receptor tyrosine kinase can be activated via gene mutation, gene amplification, protein overexpression and/or a ligand-dependent autocrine/paracrine loop [7]. c-Met, when activated in malignant cells, triggers a number of intracellular signaling transduction pathways resulting in alteration of biologic functions including metastasis [8].

It is expected that targeted therapy against c-MET and its pathway will lead to significant inhibition of cancer growth and metastasis. The expression of c-MET protein has been targeted at the RNA levels with small interference RNA, microRNA, c-MET-specific ribozymes or at the level of protein maturation. Suppression of c-MET expression by delivering small interference RNA is a novel approach. SiRNA binds to ribosomes in place of MET RNA, effectively silencing MET RNA [9-10].

Research has shown that several c-MET inhibitors are currently under investigation. Previously, a wide-spectrum kinase inhibitor at ATP binding site, K252a, was identified. Efforts to develop more specific inhibitors have led to characterization of SU11274 and PHA665752 [11]. There are a number of kinase inhibitors that have reached clinical trials [12]. These include PF2341066, XL880 (Exelixis), XL184 (Exelixis), ARQ197 (ArQule Inc.), SGX523 (SGX Pharmaceuticals), and MGCD265 (Methyl-Gene). SGX523 had to be stopped prematurely in phase I trial due to unexpected renal toxicity. Many of these inhibitors also have activity against other kinases [8]. Since the most commonly used c-Met inhibitors in NSCLC therapy present with some adverse side effect, it becomes imperative to research on an alternative drug-gable compound that offers better potency with little or no side effect.

c-Met has an increased attraction as a target for anticancer therapeutics whether in preclinical studies or clinical trials. In this study, we utilized *in-silico* approach which provided a high-quality interaction between the ligand (eugenol) and the receptor (c-Met receptor). Eugenol was then channelled to Lipinski rule of five on ADMET (Adsorption, Distribution, Metabolism, Excretion and Toxicity) properties and was found to fulfill the rule of five on ADMET properties.

MATERIALS AND METHODS

Ligand selection and preparation

The chemical structures of twenty-eight (28) phytochemicals were obtained from PubChem compound database (<https://pubchem.ncbi.nlm.nih.gov>). The MOL SDF format of these ligands were converted to PDBQT file using PyRx tool to generate atomic coordinates and energy was

minimized by optimization using the optimization algorithm at force field set at uff (required) on PyRx.

Accession and preparation of the target protein

The protein c-Met was prepared by retrieving the three-dimension crystal structure of c-Met in complex with a co-crystallized ligand (PDB:4KNB) from RCSB PDB (<http://www.rcsb.org/pdb/home/home.do>)[8]. The protein was subsequently cleaned by removing the bound complex molecule, the non-essential water molecules and all the heteroatoms using Pymol tool. The co-crystallized ligand (PDB:1RU) was extracted (not removed) from the active site so as to reveal the grid coordinate around the binding pocket when viewed on pymol.

Molecular docking using PyRx

Subsequent to receptor and ligands preparation, molecular docking analysis was performed by PyRx, AutoDock Vina option based on scoring functions. For our analysis we used the PyRx, AutoDock Vina exhaustive search docking function. After the minimisation process, the grid box resolution was centered at $16.7479 \times 0.1286 \times 23.3536$ along the x, y and z axes respectively at grid dimension of $25 \times 25 \times 25 \text{ \AA}$ to define the binding site (figure). The co-crystallized ligand which serves as the standard was first docked within the binding site of c-Met and the resulting interaction was compared with that of eugenol into the similar active sites using the same grid box dimension.

Validation of docking results

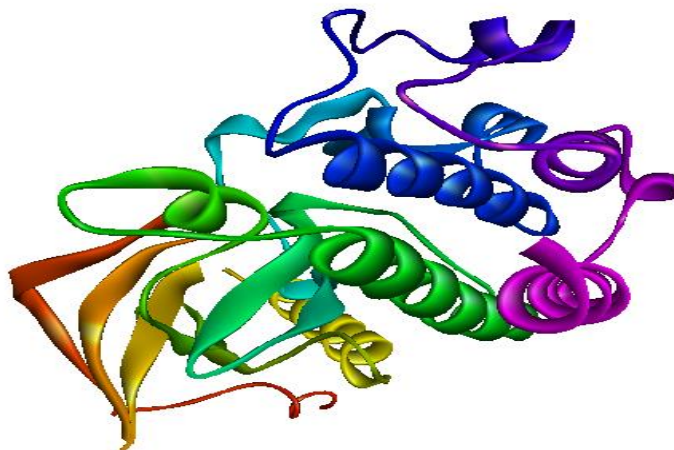
The docking results obtained were validated with the blasting of the fasta sequence of the crystal structure of the c-Met (ID: 4KNB) which was obtained from the protein data bank unto the online available ChEMBL Database (www.ebi.ac.uk/chembl/). The bioactivity generated by the database, having an activity of 287, IC50 value of 3825, and KI value of 1296, was downloaded in txt format. The bioactivity was sorted out; missing or misplaced data were removed. Only 28 of the total 3825 drug-like compounds were recovered. The compiled compounds were split and converted to 2D (in sdf format) by DataWarrior software (version 2) and converted to pdbqt format by PyRx tool. The ligands were docked into the binding domain of c-Met using PyRx AutoDock vina scoring function. A correlation coefficient graph was plotted between the docking scores of the 28 compounds generated and their corresponding PCHEMBL_VALUE (experimentally determined) values. Spearman Rank correlation coefficient graph was plotted to obtain the correlation (R^2) between the dockings results of the ChEMBL's compounds and their corresponding experimentally generated results.

RESULTS AND DISCUSSION

The Mesenchymal Epithelial Transition (MET) receptor or target belongs to a family of Receptor tyrosine kinases (RTKs). Dysregulation of the MET signaling pathway takes place in a wide range of human cancers.[13-14]. c-MET receptor is a 190 kDa glycoprotein heterodimer consisting of an extracellular α -subunit linked to transmembrane β -subunit by a disulphide bond

[15] (Fig.1).It is therefore reasonable to think that inhibiting c-Met, represents a sound pharmacological approach.

In the present study, twenty-eight (28) phytochemicals from *musa acuminata* plant were docked into the binding pocket of c-Met for their c-Met inhibitory (antagonistic) properties. Eugenol was discovered as the lead compound with the binding energy of -5.7 kcal/mol (Table 1). The drug-likeness of eugenol was assessed by subjecting it to the Lipinski's rule of five, afterwards the lead compound, eugenol violated none of the rules, this describes its bioavailability and binding potential (Table 3).



Fi

Figure 1: 3D Structure of prepared c-Met for molecular docking

Eugenol, the lead compound has a binding energy of -5.7 kcal/mol, while the standard compound has binding energy of -4.3 kcal/mol (Table 2). The highest binding energy (-5.7kcal/mol) attributed to eugenol in this regard is believed to be as a result of its chemical interactions at the receptor's active site (Table 4; Figure 4) which includes:

- Four (4) Hydrogen bonds involving LEU1225 and LEU1140 residues
- Twenty (20) Hydrophobic interactions involving LEU1140, LEU1157, ALA1221, ALA1226, LEU1225, LEU1142 and SER1141

While that of the co-crystallized ligand (PDB Ligand ID: 1RU) which serves as the standard presents with the following chemical interactions at the binding pocket (Table 5; Figure 4)

- Four (4) Hydrogen bonds involving ARG1208 and ASP1231 residues
- Eight (8) Hydrophobic interactions involving MET1211, ARG1208, TYR1230 and ASP1231 residues
- Nine (9) Electrostatic interaction involving ASP1231 and ASP1164 residues

The highest binding energy (-5.7kcal/mol) attributed to eugenol in this regard is believed to be as a result of the extensive high number of hydrophobic interactions (twenty hydrophobic

interactions) of eugenol. The average number of hydrophobic atoms in marketed drugs is 16, with one to two donors and three to four acceptors. This defines the importance of hydrophobic interactions in the design of drugs. Hydrophobic interactions can increase the binding affinity between target-drug interfaces [16].

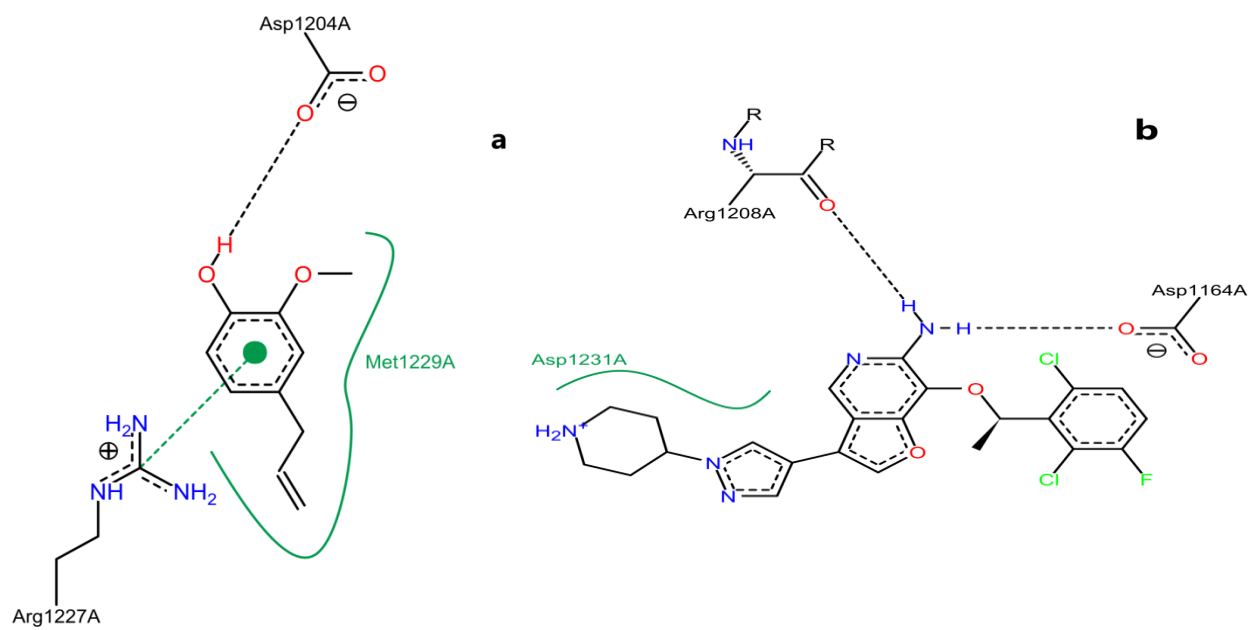


Figure 2: Pose view (a) Eugenol (b) 1RU (Co-crystallized ligand)

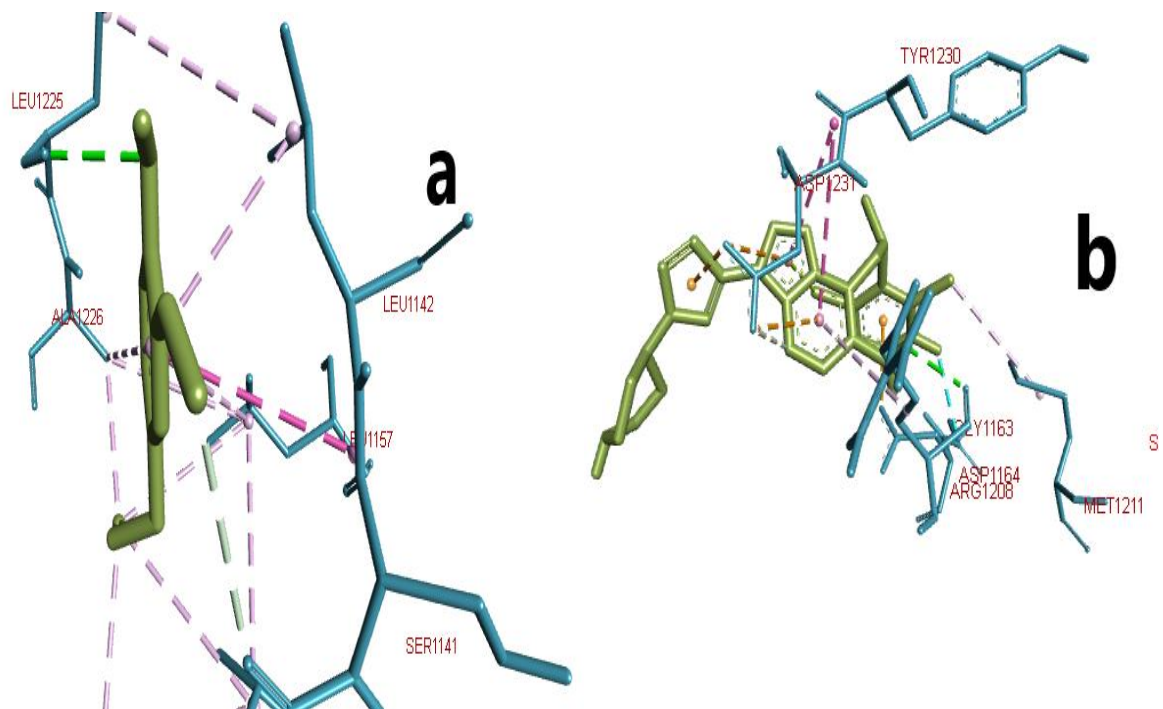
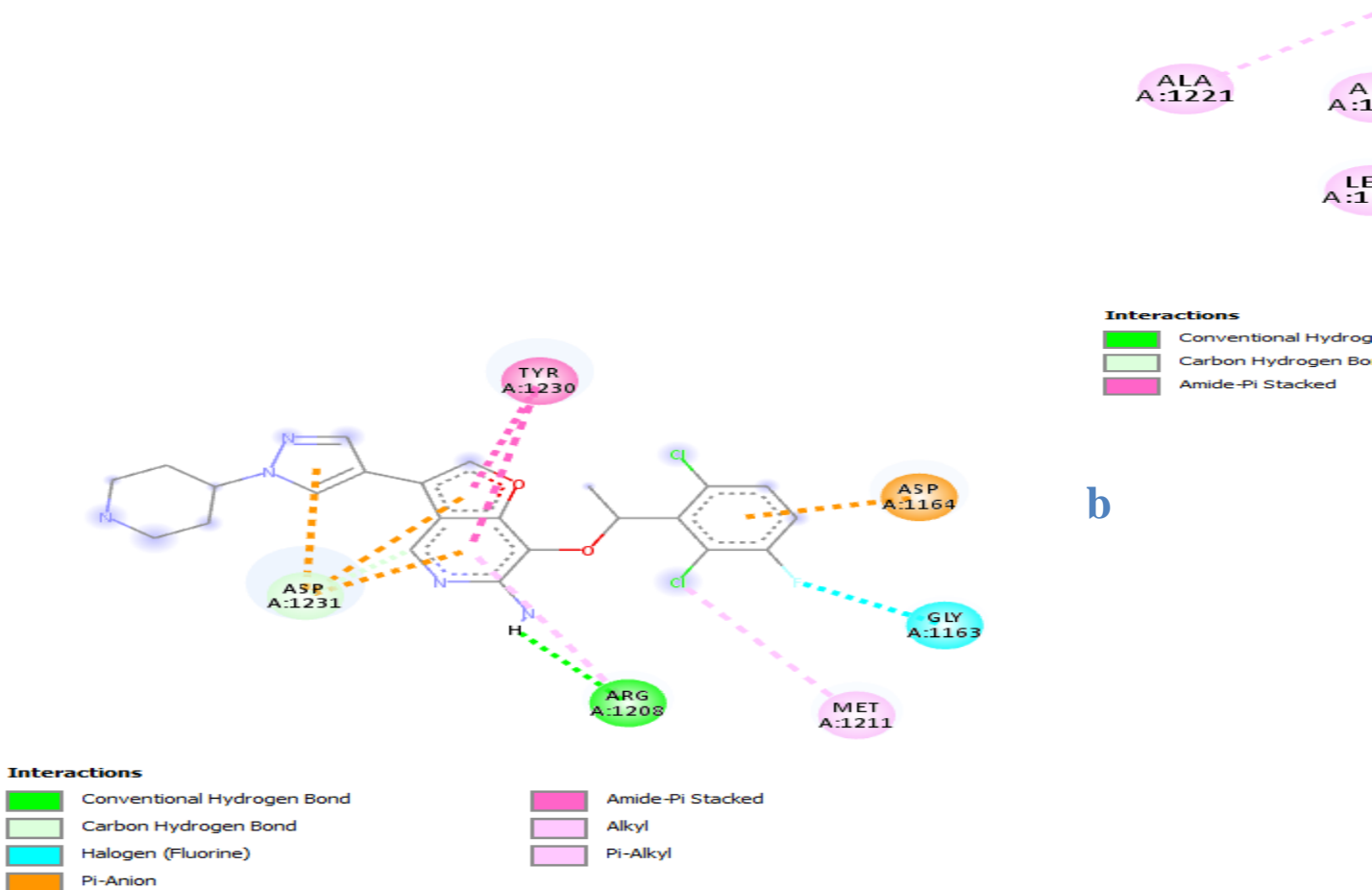


Figure 3: 3D interactions of ligands (green sticks) within the binding pocket (a) eugenol (b) 1RU

a



b

Figure 4: 2D interactions of ligands (green sticks) within the binding pocket (a) eugenol (b) 1RU

Table 1: Phytochemicals obtained from *Musa acuminata* with their respective binding energies. Eugenol has the highest docking score as compared with others.

S/N	Canonical Smiles of Compounds	Binding Energy (Kcal/mol)
1	<chem>O(c1cc(CC=C)ccc1O)C</chem>	-5.7
2	<chem>O(C(CCC)C)C(=O)C</chem>	-5.1
3	<chem>O(C(=O)CCC)CC</chem>	-5.0
4	<chem>OC1C2(CC(C1(C)C)CC2)C</chem>	-4.9
5	<chem>O(C(=O)CCC)C</chem>	-4.7
6	<chem>O(C(=O)CCC)CC</chem>	-4.7
7	<chem>O(CC(C)C)C(=O)C(C)C</chem>	-4.6
8	<chem>O(C(OCC)C)CC</chem>	-4.6
9	<chem>O(CCCCC)C(=O)C</chem>	-4.4
10	<chem>O(CCC(C)C)C(=O)CC(C)C</chem>	-4.3
11	<chem>O=C(CCCC)C</chem>	-4.3
12	<chem>O(CC(C)C)C(=O)CCC</chem>	-4.3
13	<chem>O(C(=O)CCC)C</chem>	-4.3
14	<chem>O(CC(C)C)C(=O)CCC</chem>	-4.3
15	<chem>O(CCCC)C(=O)CCC</chem>	-4.3
16	<chem>O(CCC(C)C)C(=O)CCC</chem>	-4.2
17	<chem>OC(C(=O)C)C</chem>	-4.2
18	<chem>O(C(CCC)C)C(=O)C</chem>	-4.2
19	<chem>O(CCC(C)C)C(=O)CCC</chem>	-4.2
20	<chem>O(CC(C)C)C(=O)C</chem>	-4.1
21	<chem>O(CCC)C(=O)C</chem>	-4.1
22	<chem>O(CCCCC)C(=O)C</chem>	-4.1
23	<chem>O(CC(C)C)C(=O)C</chem>	-3.9
24	<chem>O=CCCCC</chem>	-3.7
25	<chem>O=CCC(C)C</chem>	-3.6
26	<chem>OC(CCCCC)C</chem>	-3.5
27	<chem>O=C(CCCC)C</chem>	-3.4
28	<chem>OCCCC</chem>	-3.4

Table 2: Energy and RMSD values obtained during docking analysis of eugenol and the co-crystallized as ligands molecules and c-Met as target protein

S/N	Complex	Binding energy (kcal/mol)	RMS D/UB ^a	RMS D/LB ^b
1	Eugenol	-5.7	0	0

2	1RU	-4.3	0	0
RMSD/UB: Root mean square deviation/upper bond; RMSD/LB: Root mean square deviation/lower bond				

Table 3: Lipinski's drug-like properties of eugenol: The rule describes drug candidate's pharmacokinetics in the human body which also including their absorption, distribution, metabolism, and excretion ("ADME") using an online server (<http://www.scfbio-iitd.res.in/>)

Molecular Properties	Lipinski's rule of Five	Eugenol drug-like properties
Molecular Mass	<500	164.204
Hydrogen bond Acceptor	<10	2
Hydrogen bond Donor	<5	1
LogP	<5	2.198240
Molar Refractivity	Between 40-130	47.121990
Topological Polar surface .Area	<140Å ²	29.5

Table 4: Interaction table showing the various chemical interactions of eugenol within the binding pocket

S/N	Name	Category	Type
1	A:LEU1225:HN - N:1RU:O	Hydrogen Bond	Conventional Hydrogen Bond
2	N:1RU:C - A:LEU1140:O	Hydrogen Bond	Carbon Hydrogen Bond
3	A:SER1141:C,O;LEU1142:N - N:1RU	Hydrophobic	Amide-Pi Stacked
4	N:1RU:C - A:LEU1140	Hydrophobic	Alkyl
5	N:1RU:C - A:LEU1157	Hydrophobic	Alkyl
6	N:1RU:C - A:ALA1221	Hydrophobic	Alkyl
7	N:1RU:C - A:ALA1226	Hydrophobic	Alkyl
8	A:LEU1140 - A:LEU1157	Hydrophobic	Alkyl
9	A:LEU1142 - A:LEU1225	Hydrophobic	Alkyl
10	A:ALA1221 - A:LEU1140	Hydrophobic	Alkyl
11	A:ALA1226 - A:LEU1157	Hydrophobic	Alkyl
12	N:1RU - A:LEU1142	Hydrophobic	Pi-Alkyl
13	N:1RU - A:LEU1157	Hydrophobic	Pi-Alkyl
14	N:1RU - A:ALA1226	Hydrophobic	Pi-Alkyl
15	A:LEU1225:HN - N:1RU:O	Hydrogen Bond	Conventional Hydrogen Bond
16	N:1RU:C - A:LEU1140:O	Hydrogen Bond	Carbon Hydrogen Bond
17	A:SER1141:C,O;LEU1142:N - N:1RU	Hydrophobic	Amide-Pi Stacked
18	N:1RU:C - A:LEU1140	Hydrophobic	Alkyl
19	N:1RU:C - A:LEU1157	Hydrophobic	Alkyl
20	N:1RU:C - A:ALA1221	Hydrophobic	Alkyl
21	N:1RU:C - A:ALA1226	Hydrophobic	Alkyl
22	N:1RU - A:LEU1142	Hydrophobic	Pi-Alkyl
23	N:1RU - A:LEU1157	Hydrophobic	Pi-Alkyl
24	N:1RU - A:ALA1226	Hydrophobic	Pi-Alkyl

Table 5: Interaction table showing the chemical interactions of the co-crystallized ligand within the binding pocket

S/N	Name	Category	Types
1	N:1RU:H - A:ARG1208:O	Hydrogen Bond	Conventional Hydrogen Bond
2	N:1RU:C - A:ASP1231:OD2	Hydrogen Bond	Carbon Hydrogen Bond
3	A:GLY1163:C - N:1RU:F	Halogen	Halogen (Fluorine)
4	A:ASP1164:OD1 - N:1RU	Electrostatic	Pi-Anion
5	A:ASP1231:OD1 - N:1RU	Electrostatic	Pi-Anion
6	A:ASP1231:OD1 - N:1RU	Electrostatic	Pi-Anion
7	A:ASP1231:OD2 - N:1RU	Electrostatic	Pi-Anion
8	N:1RU:Cl - N:1RU	Other	Pi-Lone Pair
9	A:TYR1230:C,O;ASP1231:N - N:1RU	Hydrophobic	Amide-Pi Stacked
10	A:TYR1230:C,O;ASP1231:N - N:1RU	Hydrophobic	Amide-Pi Stacked
11	N:1RU:Cl - A:MET1211	Hydrophobic	Alkyl
12	N:1RU - A:ARG1208	Hydrophobic	Pi-Alkyl
13	N:1RU:H - A:ARG1208:O	Hydrogen Bond	Conventional Hydrogen Bond
14	N:1RU:C - A:ASP1231:OD2	Hydrogen Bond	Carbon Hydrogen Bond
15	A:GLY1163:C - N:1RU:F	Halogen	Halogen (Fluorine)
16	A:ASP1164:OD1 - N:1RU	Electrostatic	Pi-Anion
17	A:ASP1231:OD1 - N:1RU	Electrostatic	Pi-Anion
18	A:ASP1231:OD1 - N:1RU	Electrostatic	Pi-Anion
19	A:ASP1231:OD2 - N:1RU	Electrostatic	Pi-Anion
20	N:1RU:Cl - N:1RU	Other	Pi-Lone Pair
21	A:TYR1230:C,O;ASP1231:N - N:1RU	Hydrophobic	Amide-Pi Stacked
22	A:TYR1230:C,O;ASP1231:N - N:1RU	Hydrophobic	Amide-Pi Stacked
23	N:1RU:Cl - A:MET1211	Hydrophobic	Alkyl
24	N:1RU - A:ARG1208	Hydrophobic	Pi-Alkyl

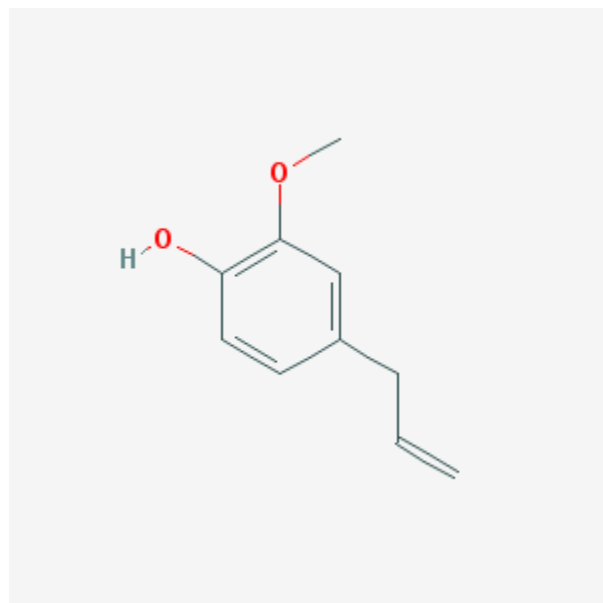


Figure 4: Structure of Eugenol

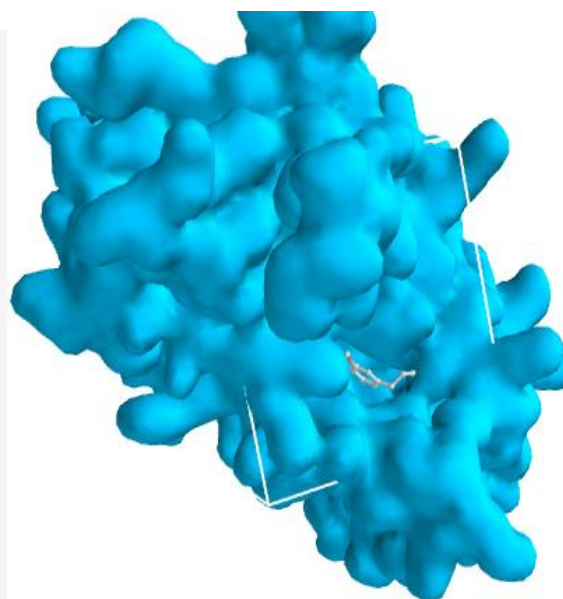


Figure 5: Grid box within which the ligand binds. 16.7479x 0.1286 x 23.3536 along the X, Y, Z axis

We validated the accuracy of our docking protocol by redocking eugenol back into the binding pocket of the c-Met (4KNB). As stated, the re-docked pose overlapped almost totally with the experimental orientation, indicating that Autodock vina on PyRx re-docked eugenol, with a very high accuracy, back into the binding pocket of the c-Met, this reveals that our docking methodology was reliable and the docking scores obtained are correct (Figure 6).

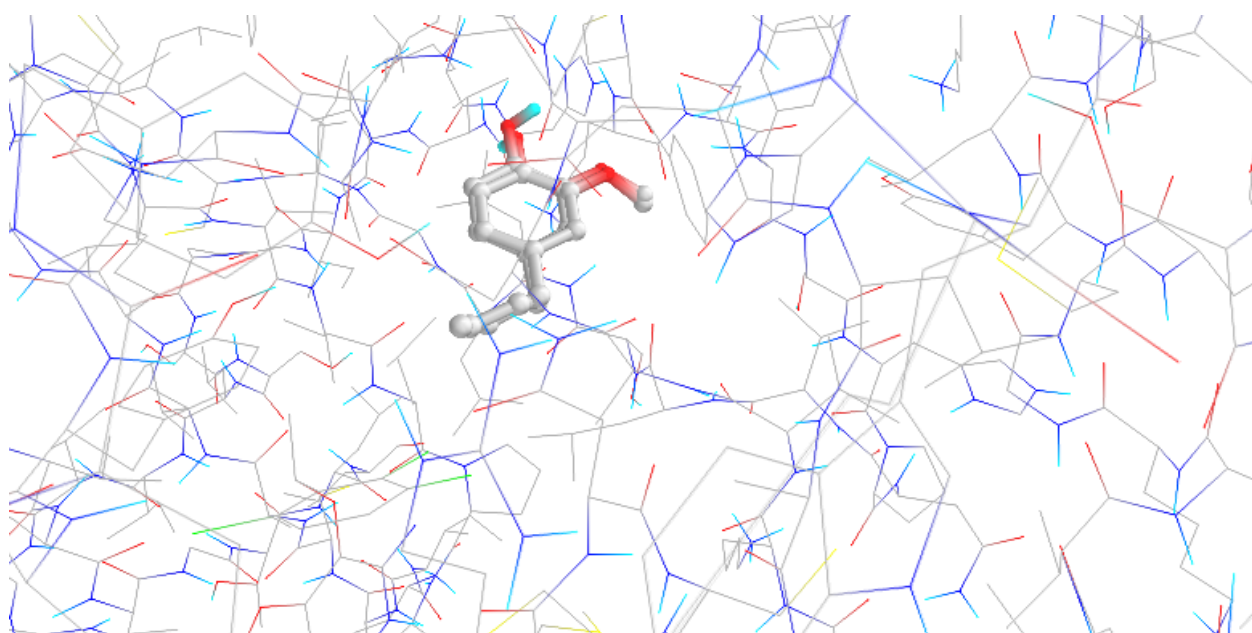


Figure 6: Validation of docking: Comparability of the re-docked binding mode and the pose of eugenol with the accompany residues of c-Met binding pocket. A snapshot from PyRx

The reliability of our docking scores was further validated using the online available ChEMBL Database, the Fasta sequence of the crystal structure of c-Met (ID: 4KNB) was blasted on www.ebi.ac.uk/chembl/. The compounds obtained from the search were docked into the binding site of the c-Met, a correlation coefficient graph plotted between the docking scores of the compounds generated and their corresponding ChEMBL's Pchem values (experimentally determined IC₅₀). This showed a strong correlation coefficient ($R^2=0.823$) between the docking scores and the experimentally derived data in the present study which gave credence to the fact that computational experiment can replicate experimental data at least in this present study and that our docking scores, using PyRx AutoDock Vina algorithm is dependable (Figure 7).

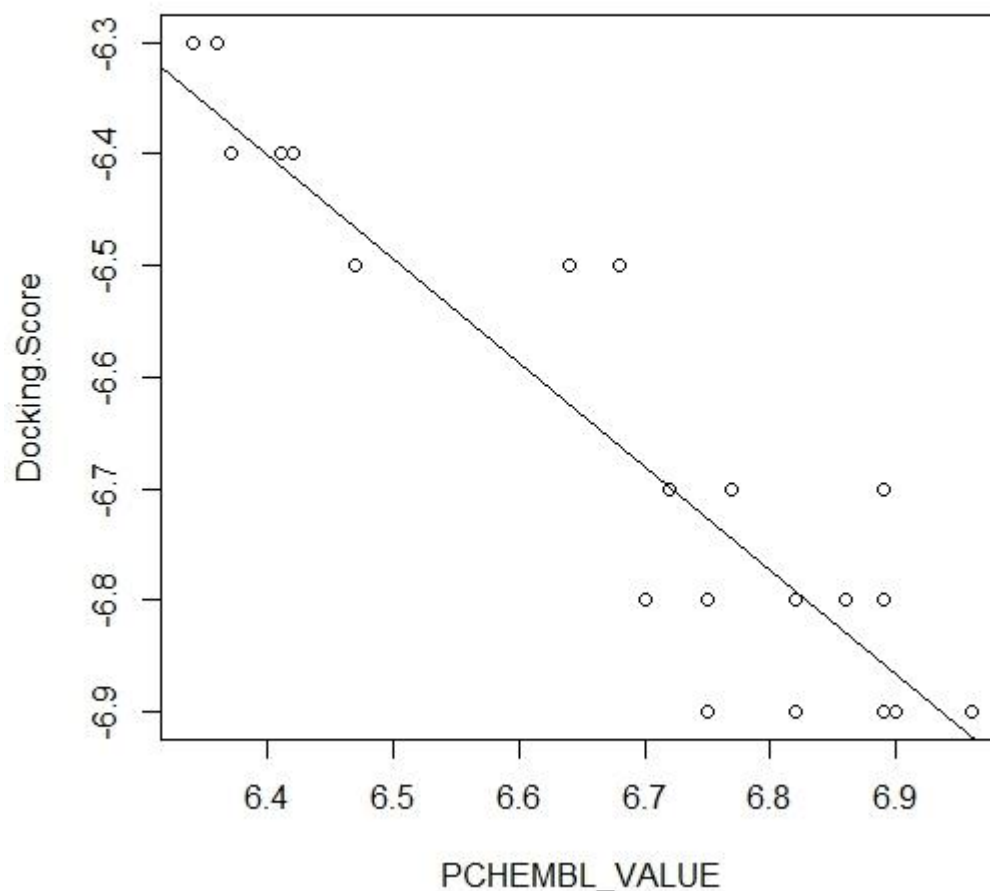


Figure 7: Correlation coefficient graph of docking scores of various antagonists of the c-Met and their corresponding experimental pIC50 (pchembl_values) values. The antagonists (compounds) and their corresponding pIC50 (experimentally derived IC50) were downloaded from the ChemBL database, the strong correlation (0.823) between the docking scores and pIC50 shows that computer can reproduce experimental values and this gives credence to the docking scores generated, in the present study.

CONCLUSION

Docking studies and ADMET evaluation of eugenol with c-Met showed that this ligand is a drug-gable molecule which docks well with c-Met target. Therefore, eugenol molecule plays an important role in inhibiting c-Met and thus should be implicated as a potential agent in cancer therapy.

REFERENCES

1. Dela Cruz, C. S., Tanoue, L. T. & Matthay, R. A. Lung cancer: epidemiology, etiology, and prevention. *Clinics in chest medicine* **32**, 605–644 (2011).
2. Torre, L. A. *et al.* Global cancer statistics, 2012. *CA: a cancer journal for clinicians* **65**, 87–108 (2015).
3. Travis, W. D. *et al.* The 2015 World Health Organization Classification of Lung Tumors: Impact of Genetic, Clinical and Radiologic Advances Since the 2004 Classification. *Journal of thoracic oncology: official publication of the International Association for the Study of Lung Cancer* **10**, 1243–1260 (2015).
4. Ye, S. *et al.* The Efficacy and Risk Profile of c-Met inhibitors in Non-small Cell Lung Cancer: a Meta-analysis. *Sci. Rep.* **6**, 35770; doi: 10.1038/srep35770 (2016).
5. Jeffers M, Rong S, Vande Woude GF (1996) Enhanced tumorigenicity and invasion-metastasis by hepatocyte growth factor/scatter factor-met signalling in human cells concomitant with induction of the urokinase proteolysis network. *Mol Cell Biol* **16**: 1115–1125
6. PC Ma, MS Tretiakova, V Nallasura, R Jagadeeswaran, AN Husain² and R Salgia. Downstream signalling and specific inhibition of c-MET/HGF pathway in small cell lung cancer: implications for tumour invasion. *British Journal of Cancer* (2007) **97**, 368–377. doi:10.1038/sj.bjc.6603884
7. Neelesh Sharma and Alex A. Adjei. In the clinic: ongoing clinical trials evaluating c-MET-inhibiting drugs. *Ther Adv Med Oncol* (2011) **3**(S1) S37_S50 DOI: 10.1177/
8. Eric S. Kim and Ravi Salgia. MET Pathway as a Therapeutic Target. *J Thorac Oncol.* **2009**;4: 444–447
9. Kuhn DE, Martin MM, Feldman DS, Terry AV Jr, Nuovo GJ, Elton TS. Experimental validation of miRNA targets. *Methods* **2008**;44:47–54.
10. Ross JS, Carlson JA, Brock G. miRNA: the new gene silencer. *Am J Clin Pathol* **2007**;128:830–836.
11. Morotti A, Mila S, Accornero P, Tagliabue E, Ponzetto C. K252a inhibits the oncogenic properties of Met, the HGF receptor. *Oncogene* **2002**;21:4885–4893.
12. Abidoye O, Murukurthy N, Salgia R. Review of clinic trials: agents targeting c-Met. *Rev Recent Clin Trials* **2007**;2:143–147.

13. Peters S, Adjei AA. MET: a promising anticancer therapeutic target. *Nat Rev Clin Oncol*. 2012;9(6):314–26.
14. Ma roun CR, Rowlands T. The Met receptor tyrosine kinase: a key player in oncogenesis and drug resistance. *Pharmacol THer*. 2014;142(3):316–38.
15. Gara jová et al. c- Met as a Target for Person alized Th erapy. *Translat ional Oncogenomics* 2015;7(S1) 13-31
16. Rohan Patil, Suranjana Das, Ashley Stanley, Lumbani Yadav, Akulapalli Sudhakar, Ashok K. Varma *PLoS One*. 2010; 5(8): e12029. Published online 2010 Aug 16. doi: 10.1371/journal.pone.0012029 PMCID: PMC2922327
17. K. P. Sampath Kumar, Debjit Bhowmik, S.Duraivel and M.Umadevi. Tradtional uses of banana. *Journal of pharmacognosy and phytochemistry*. 1(3), 2012. ISSN 2278-4136